Charge-Gating Dibenzothiophene-*S*,*S*-Dioxide Bridges in Electron Donor–Bridge–Acceptor Conjugates

Gilles Yzambart,[a,II] *Anna Zieleniewska,*[b,II] *Stefan Bauroth,*[b] *Timothy Clark,*[c] *Martin R. Bryce,**[a] *Dirk M. Guldi**[b]

[a] Department of Chemistry, Durham University, Durham DH1 3LE, United Kingdom.

[b] Department of Chemistry and Pharmacy & Interdisciplinary Center for Molecular Materials, Friedrich-Alexander-Universität Erlangen-Nürnberg, Egerlandstr. 3, 91058 Erlangen, Germany.

[c] Computer-Chemie-Centrum & Interdisciplinary Center for Molecular Materials, Department of Chemistry and Pharmacy, Friedrich-Alexander-Universität Erlangen-Nürnberg, Nägelsbachstr. 25, 91052 Erlangen, Germany.

[II] These authors contributed equally.

AUTHOR EMAIL ADDRESS: m.r.bryce@durham.ac.uk; guldi@chemie.uni-erlangen.de

RECEIVED DATE (to be automatically inserted after your manuscript is accepted if required according to the journal that you are submitting your paper to)

CORRESPONDING AUTHOR FOOTNOTE: Prof. Dr. Martin R. Bryce, Department of Chemistry, Durham University, Durham DH1 3LE, United Kingdom. Phone: +41 (0)191 334 2018, fax: +41 (0)191 384 4737, email: m.r.bryce@durham.ac.uk; Prof. Dr. Dirk M. Guldi, Department of Chemistry and Pharmacy & Interdisciplinary Center for Molecular Materials (ICMM), Friedrich-Alexander-Universität Erlangen-Nürnberg, Egerlandstr. 3, 91058 Erlangen, Germany, phone: +49 9131 8527341, fax: +49 9131 85-28307, email: dirk.guldi@fau.de

ABSTRACT: The synthesis of a series of new electron donor–bridge–acceptor (D–B–A) conjugates (**18-20**) comprising electron-donating zinc(II)porphyrins (ZnP) and electron-accepting fullerenes (C_{60}) connected through various co-oligomer bridges containing both dibenzothiophene-*S,S*-dioxide (S) and fluorene (Fl) units is reported. Detailed investigations using cyclic voltammetry, absorption, fluorescence, and femto/nanosecond transient absorption spectroscopy in combination with quantum chemical calculations have enabled us to develop a detailed mechanistic view of the charge-transfer processes that follow photoexcitation of either ZnP, the bridge or C_{60}. Variations in the dynamics of charge separation, charge recombination, and charge transfer gating are primarily consequences of the electronic properties of the co-oligomer bridges, including its electron affinity and the energy levels of the excited states. In particular, placing one dibenzothiophene-*S,S*-dioxide building block at the center of the molecular bridge flanked by two fluorene building blocks, as in **20**, favors hole- rather than electron-transfer between the remote electron donors and acceptors, as demonstrated by exciting C_{60} rather than ZnP. In **18** and **19**, in which one dibenzothiophene-*S,S*-dioxide and one fluorene building block constitute the molecular bridge, photoexcitation of either ZnP or C_{60} results in both hole- and electron transfer. Dibenzothiophene-*S,S*-dioxide is thus shown to be an excellent building block for probing how subtle structural and electronic variations in the bridge affect unidirectional charge transport in D–B–A conjugates. The experimental results are supported by computational calculations.

Introduction

Covalent electron donor–bridge–acceptor (D–B–A) conjugates provide valuable insight into unimolecular charge-transport dynamics that allow their use in molecular and optoelectronic devices, solar energy conversion, and nanoscale applications such as information storage.[1-11] These studies are also important as models for the stepwise charge-transfer processes in complex naturally occurring systems, such as the photosynthesis reaction center.[12-15]

It is, therefore, of paramount importance to understand the effects of systematically varying the chemical structure and length of the bridge in new D–B–A systems, where the bridge mediates the electronic coupling between donor- and acceptor moieties over large distances.[4,16-24] Coupling typically decays exponentially with increasing distance between the D and A termini,[25] as reflected by the electron-transfer rate constant k_{ET}. Thus, the rates of charge separation and recombination are characterized by

$$k_{ET} = k_0 e^{-\beta R_{DA}} \quad (1)$$

where k_0 is a kinetic pre-factor, R_{DA} is the electron donor-acceptor distance and β is the attenuation factor, which varies with the intrinsic electronic properties of the bridge. The value of β should be low for efficient and rapid charge-transfer reactions. Generally, low β requires a high degree of conjugation across the entire D–B–A system, i.e. a homogeneously conjugated molecular bridge and efficient electronic coupling of the bridge to the terminal D and A units. Note, however, that π-conjugated bridges exhibit a transition in the charge-transfer mechanism from coherent transfer to hopping at longer bridge lengths.

Gating charge transfer has been demonstrated upon chemical or conformational modification of the π-conjugated bridges. For example, when [2,2′]-paracyclophanes are introduced into oligo-*p*-phenylenevinylene bridges, their through-space π-π interactions have a large effect on the charge-transport properties. Selective photoexcitation of either D or A enables unidirectional charge transfer in the form of holes from A to D, but suppresses it from D to A.[26] Likewise, significant flexibility of oligo-

p-phenylenevinylenes affects the charge transfer. Temperature-dependent experiments have shown that charge separation is gated by torsional motions, which are operative between an electron-donating tetracene and the first bridge phenyl ring. Charge recombination in multiple phenyl-vinyl linkages has also been found to be temperature dependent.[27]

Many different molecular bridges have been used to link D-A conjugates. Representative examples are oligo-phenylenevinylenes (oPVs),[28-32] oligo-phenyleneethynylenes (oPEs),[32-39] oligo-fluorenes (oFls),[40-43] oligo-vinylfluorenes,[44] ladder-OFls,[45] oligo-ynes,[46-49] oligo-thiophenes,[50-53] oligo-vinylthiophenes,[54] oligo(ethynylene-10,20-porphyrindiyl-ethynylene)s,[55] oligo-phenylenes,[56-60] and others.[61,62] It should be noted that different β-values have been reported for the same bridge connected either to different Ds and As, or to the same Ds and As via different linking units.[63] In both cases, the key feature is the extent of matching/mismatching of the donor-bridge and acceptor-bridge energy levels, which modify the π–conjugation pathway.

Fluorene is a very effective π–conjugating molecular wire;[64] the attenuation factor of oFl bridges[40-43] lies between those of oPVs and oPEs. This property renders oFls ideal building blocks for fine tuning electronic properties by systematic structural changes. Indeed, this feature of fluorene has been widely recognized in the design of semiconducting materials for organic light-emitting devices and photovoltaic cells, in which co-oligomers and co-polymers of fluorene with other π–conjugated monomer units, for example electron-deficient benzothiadiazole[65-67] or dibenzothiophene-*S,S*-dioxide (S),[68-74] are used to modulate charge transport.

The objective of this work is to synthesize and study the photophysical properties of new ZnP–B–C_{60} (ZnP = zinc(II)porphyrin) conjugates that incorporate both fluorene (Fl) and dibenzothiophene-*S,S*-dioxide (S) building blocks in the molecular bridge. A co-oligomer approach has been remarkably effective in terms of the synthetic design of π-conjugated polymers. Addition of electron-rich or electron-poor substituents to the polymer backbone respectively, assists in increasing or

decreasing the acceptor or donor energy levels. For example, polymers containing boron received great attention due to their excellent performance: both donor and

acceptor energy levels are lowered by more than 0.5 eV, as shown by the increased electron affinity.[75,76] Such a strategy, however, with co-oligomer units in the bridge has not been explored previously in D–B–A conjugates. Fl and S are topologically very similar, so that replacing Fl by S should have minimal effect on the length and conformation of the resulting bridges. The impact of the electron-withdrawing nature of the S unit on the photoinduced charge-transfer properties in D–B–A conjugates can therefore be explored. We are aware of only one detailed report of the incorporation of electron-deficient building blocks into the bridge of D–B–A conjugates: ZnP–B–C_{60} conjugates with a diphenyl-1,2,3-triazole bridge. In particular, changes in the electronic coupling were found to depend on the different connectivity at the central 1,2,3-triazole unit and to alter the charge-transfer dynamics but not gate the charge transfer.[77] Reference 77 therefore differs from the present work, in which the special molecular feature is that the dibenzothiophene-*S,S*-dioxide unit is placed at different positions in the bridge, with the same connectivity at the S and Fl units in all cases. Such a strategy enables insights into the influence of electron-deficient building blocks in oligomeric bridges in terms of modulating and gating charge transfer in D-B-A conjugates. ZnP and C_{60} were selected as electron donors and acceptors, respectively, based on their unique features in D–B–A conjugates.[40,77,78] Most importantly, the small reorganization energies in electron transfer reactions place the charge separation and recombination far from the maximum of the Marcus parabola into the normal and inverted regions, respectively. Based on the aforementioned the ways and means are ensured to measure accurately and to evaluate both the charge separation and the charge recombination dynamics.

Results and Discussion

Synthesis. A series of ZnP–bridge–C_{60} conjugates was synthesized. The target D–B–As **18-20** were compared with previously reported reference ZnP–$(Fl)_n$–C_{60} conjugates **21** and **22**, which feature all-Fl bridges.[41]

The synthesis of the bridges is shown in Scheme 1. The strategy included attaching boronic ester and formyl groups at the terminal positions of the bridge for subsequent linking to ZnP and C_{60}, respectively. The initial attempt to convert dibromodibenzothiophene-*S*,*S*-dioxide (Br-S-Br) **1**[68] into **2** using *n*-BuLi solution in hexane at −78 ^{o}C followed by addition of *N*,*N*-dimethylformamide (DMF) gave a mixture of products. ^{1}H NMR spectra showed the presence of formyl groups, but **2** could not be isolated. Following the procedure reported by Davies *et al.* for dibromobiphenyl,[79] a metal-halogen exchange reaction on **1** was performed at 0 ^{o}C using lithium tri-*n*-butylmagnesiate, prepared *in situ*, followed by addition of DMF to afford the desired mono-formylated product **2** in 72% yield. Next, Suzuki-Miyaura cross-coupling reactions between Br-S-CHO **2** and fluorenediboronic ester BE-Fl-BE **3**[80] gave BE-Fl-S-CHO **4** in 34% yield, which was separated by chromatography from the symmetrical dialdehyde **5** (6% yield). In a similar way, 3 equivalents of Br-S-Br **1** and BE-Fl-CHO **6**[81] gave Br-S-Fl-CHO **7** in 81% yield together with the symmetrical dialdehyde derivative (OHC-Fl-S-Fl-CHO) **8** in low yields. The yield of **8** was increased to 83% following another process described in the Supporting Information. Br-S-Fl-CHO **7** was then reacted with bis(pinacolato)diboron to afford BE-S-Fl-CHO **9**, which decomposed on attempted purification, and was therefore used directly in the next step. The ^{1}H NMR spectrum of the crude product **9** showed no evidence for the presence of any unreacted starting material **7**, which, if present, could compete with **11** in the next step of the reaction sequence. Reaction of **7** with BE-Fl-BE **3** gave BE-Fl-S-Fl-CHO **10** (52% yield).

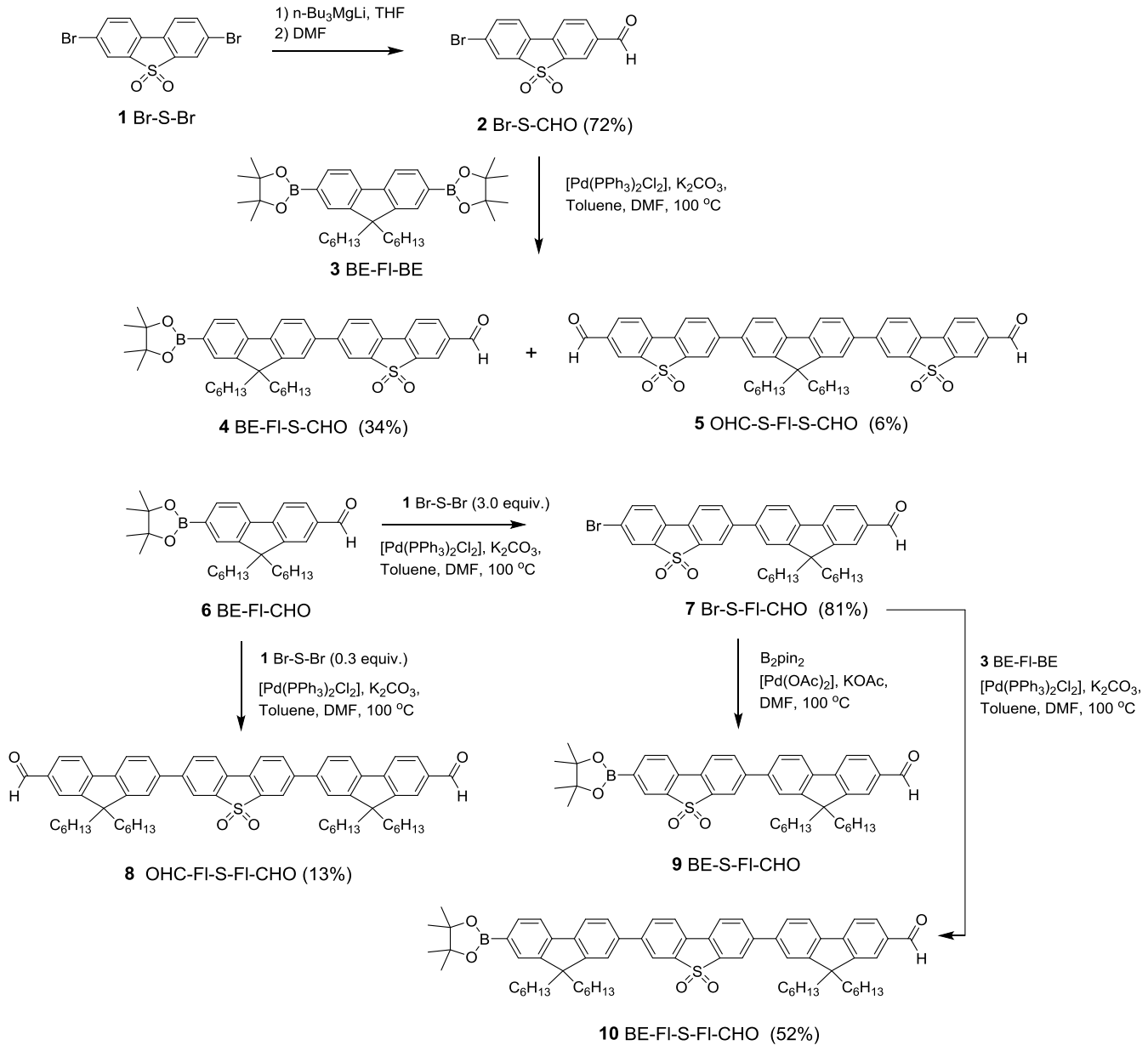

Scheme 1. Synthesis of molecular bridges incorporating both fluorenes (Fl) and dibenzothiophene-*S*,*S*-dioxides (S).

Porphyrin (H_2P) was attached to the bridges using a cross-coupling reaction between 5-(4-bromophenyl)-10,15,20-tris(4-*t*-butylphenyl)porphyrin **11**[41] and the boronic ester group of the bridges **4**, **9**, or **10** to give the H_2P-Ph-bridge-CHO derivatives **12-14**, in 52%, 10%, and 61% yields, respectively (Scheme 2). The low yields of **13** are because aldehyde **9** could not be obtained pure (*vide supra*). Upon refluxing **12-14** with zinc acetate in chloroform, the corresponding zinc porphyrins ZnP-Ph-Fl-S-CHO

(**15**), ZnP-Ph-S-Fl-CHO (**16**), and ZnP-Ph-Fl-S-Fl-CHO (**17**) were obtained as purple powders in high yields. These were then attached to C_{60} in the form of fulleropyrrolidines using Prato conditions[82,83] of the *in situ* generated azomethine ylides, which afforded the target D–B–As ZnP-Ph-Fl-S-C_{60} (**18**), ZnP-Ph-S-Fl-C_{60} (**19**), and ZnP-Ph-Fl-S-Fl-C_{60} (**20**) in 65%, 89%, and 70% yields, respectively. Full experimental details and NMR and mass spectra are provided in the Supporting Information. The structures of references **21**,[41] **22**,[41] **23**, and **24**, which were used in the electrochemical and photophysical characterizations are shown in Chart 1 and the synthesis of **23** and **24** is reported in the Supporting Information.

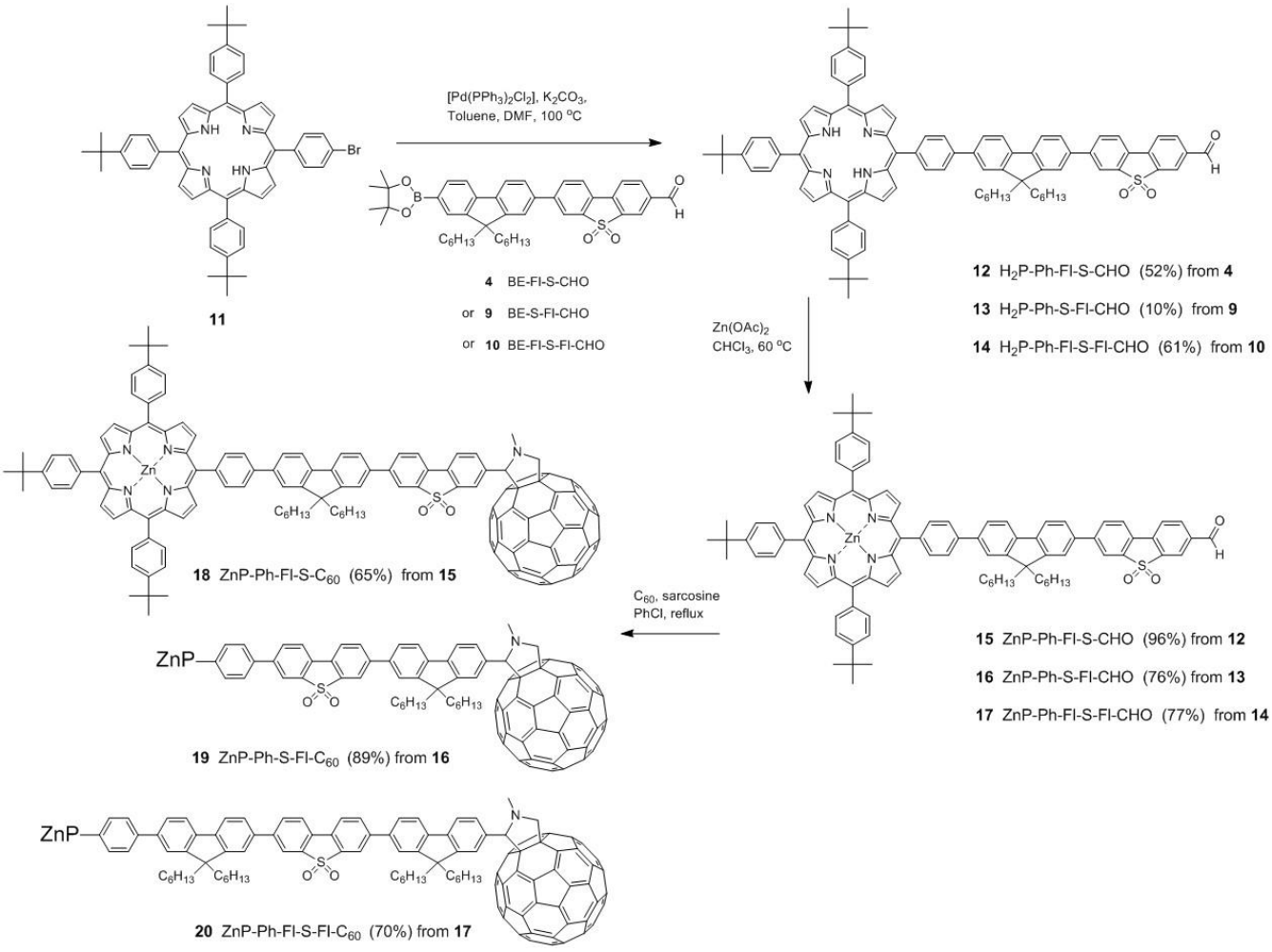

Scheme 2. Synthesis of ZnP-bridge-C_{60} conjugates.

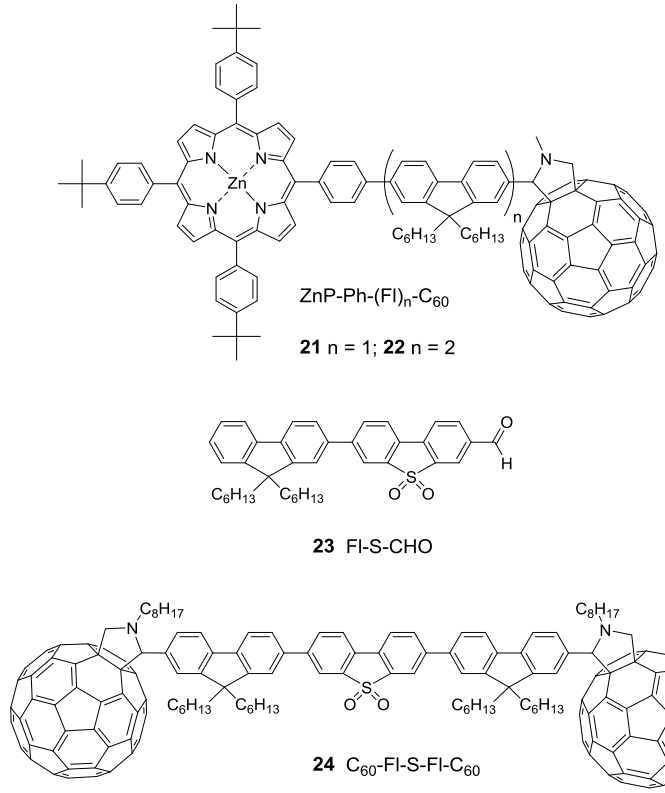

Chart 1. Model compounds used in this work.

Solution Electrochemical Studies. The redox properties of the D–B–As and their references were studied by cyclic voltammetry (CV) and differential pulse voltammetry (DPV) (Figure S1). The relevant CV and DPV data are summarized in Table 1.

Table 1. Electrochemical data.[a]

Compound	$E^5_{1/2red}$	$E^4_{1/2red}$	$E^3_{1/2red}$	$E^2_{1/2red}$	$E^1_{1/2red}$	$E^1_{1/2ox}$	$E^2_{1/2ox}$	$E^3_{1/2ox}$
Fl-S-CHO (**23**)			-2.24	-2.11	-1.74	1.26		
OCH-Fl-S-Fl-CHO (**8**)			-2.27	-2.15	-2.07	1.28		
C_{60}-Fl-S-Fl-C_{60} (**24**)		-2.08	-1.98	-1.45	-1.04	0.84		
ZnP-Ph-Fl-S-CHO (**15**)		-2.17	-2.11	-1.80	-1.71	0.34	0.70	
ZnP-Ph-S-Fl-CHO (**16**)				-2.12	-1.80	0.32	0.71	0.96
ZnP-Ph-Fl-S-Fl-CHO (**17**)			-2.14	-2.07	-1.80	0.31	0.69	1.18
ZnP-Ph-Fl-S-C_{60} (**18**)	-2.27	-1.99	-1.82	-1.46	-1.08	0.31	0.68	
ZnP-Ph-S-Fl-C_{60} (**19**)	-2.13	-2.02	-1.80	-1.46	-1.07	0.29	0.71	0.93
ZnP-Ph-Fl-S-Fl-C_{60} (**20**)	-2.15	-2.06	-1.84	-1.51	-1.12	0.30	0.68	1.13
ZnP			-2.20	-2.03	-1.83	0.34	0.72	0.92
N-methylfullerenopyrrolidine			-2.05	-1.52	-1.13			

[a] Potentials are reported in V (half-wave potentials: $E_{1/2}$); scan rate 100 mV s^{-1}. Measurements were performed at room temperature in dichloromethane containing 0.1 M $TBAPF_6$ as supporting electrolyte with a glassy carbon as the working electrode, a platinum counter electrode, and Ag-wire as a quasi-

reference electrode. The values are corrected for ferrocene as an internal standard. The peak potentials obtained from the DPV measurements were converted to $E_{1/2}$ values using the formula $E_{max} = E_{1/2} - (\Delta E/2)$, in which ΔE is the pulse amplitude (25 mV).

Using [5,10,15,20-tetrakis(4-*t*-butylphenyl)porphyrin]Zn (ZnP), *N*-methylfulleropyrrolidine (C_{60}), **8**, and **23** as references allowed us to assign the individual redox steps. For **24**, four consecutive quasi-reversible reductions were observed, which are assigned to reductions of C_{60}. Because the two C_{60}-fullerenes are electronically independent, each reduction corresponds to a two-electron process. In accordance with C_{60}-dumbbells investigated previously, hardly any electronic communication between the two fullerenes is found in room temperature experiments.[81] Upon closer analysis of D–B–As **18**-**20**, five quasi-reversible reductions were observed. The first, second and fourth reductions are centered on C_{60} and the third is assigned to ZnP and the fifth to the corresponding bridge. Analyses of the CV measurements of **15**-**17** revealed similar trends, with the exception that C_{60}-centered reductions are absent. For **16** and **17**, the first reductions are in good agreement with those seen in the ZnP reference. In contrast, the first reduction of **15** is assigned to the F-S unit by comparison with **23**. All the remaining reductions of **15**-**17** involve either ZnP or the corresponding bridges. Overall, the resemblance of the individual reductions between the D–B–As and their references indicates no significant electronic interactions among the individual constituents in the ground state.

The first two oxidation processes for **15** and **17**, and the three for **16** are in sound agreement with those found for ZnP. The third oxidation in **17** is attributed to a bridge-centered step, as also seen in **8**. Likewise, several quasi-reversible processes were observed for D–B–As **18**-**20**. Here, the first two oxidations are attributed to processes involving ZnP. The third oxidation in the case of **19** is in good agreement with the ZnP reference. In contrast, the third oxidation in **20** is assigned to the Fl-S-Fl bridge. However, the latter is shifted cathodically by 150 mV compared to the first oxidation of diformyl derivative **8** because of the conjugation between the electron-withdrawing formyl groups and the Fl-S-Fl, whose oxidation potential is accordingly higher. Perepichka *et al.* observed that the incorporation of S into an oligofluorene bridge results in a substantial reduction in the energy gap.[68] Our own

investigations reveal a similar behavior, which is particularly pronounced in **23** in comparison to Fl-Fl-CHO. In short, the presence of the electron deficient S in the bridge leads to a decrease in the energy gap by 324 mV for **23** and by 55 and 85 mV for **18** and **19**, respectively, compared with previously reported analogs without the S unit.[41]

Independent confirmation for the lack of significant ground-state interactions came from density-functional theory (DFT) calculations at the B3LYP[84]/cc-pVDZ[85] level of theory. In particular, the natural population analysis (Table S4), the almost unaffected molecular orbital energies (Figure S14) and the ground state electrostatic potential map (Figure S17) are all unperturbed relative to the reference porphyrin and fullerene. This, in combination with the unchanged electrochemical redox potentials, allows us to conclude that no significant electron or charge transfer is present in ground state. However, molecular orbitals (Figure S14-S15) are delocalized, as in **18**, **19**, and **20** the two lowest unoccupied orbitals of the ZnP-moiety, which are degenerate in the unperturbed porphyrin, are split by 15 meV by interactions with the bridge. Additionally, the ZnP-centered HOMO and the fullerene-centered occupied molecular orbitals show bridge contributions. This in particular suggests the potential for superexchange-assisted electron- or hole-transfer in the excited state.

Local electron affinity[86] and local ionization potential maps based on semiempirical AM1*[87] calculations provide insight[88] into the electronic properties of the different bridges (Figure 1). In stark contrast to fluorene bridges lacking dibenzothiophene-*S,S*-dioxide, where the electron affinity assumes uniform values along the bridges, the presence of the latter introduces a 15 kcal mol^{-1} higher electron affinity. The local ionization potential of the fluorenes supports their better electron-donating properties. The local-property maps suggest the existence of bridge-centered charge-transfer states, based on the high electron affinity of the S unit.

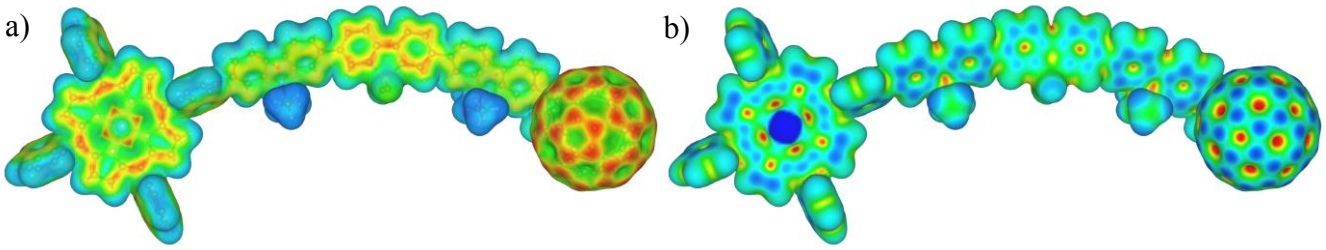

Figure 1. Local properties projected onto the 0.05 $e^{-}Å^{-3}$ isodensity surface of **20**: a) local electron affinity; the color scale ranges from -130 (blue) to 10 kcal mol^{-1} (red): b) local ionization potential; the color scale ranges from 330 (blue) to 550 kcal mol^{-1} (red).

Photophysics. The absorption spectrum of **24** is best described as the sum of the absorption spectra of **8** and C_{60} (Figure S2a). Evidence for the presence of C_{60} stems from a strong 255 nm absorption and a weak 431 nm absorption, whereas that for **8** is based on the 370 nm maximum. The absorption spectra of D–B–As **18-20** can be compared to those of the reference compounds **15-17** in order to characterize the electronic ground states. The spectra of **15-17** are dominated in the visible by the Soret and Q-bands of ZnP at 426 nm and 550/591 nm, respectively (Figure S2b), and in the UV by bridge absorptions between 300 and 390 nm. The presence of C_{60} in D–B–As **18-20** does not result in appreciable shifts (Figure S2c). A comparison of the absorption spectra of the different conjugates with their individual components does not reveal significant electronic interactions in the ground states. This is in line with vertical excitation energies calculated by TD-B3LYP[89,90]/cc-pVDZ and additional configuration interaction singles calculations (CIS) with the AM1* Hamiltonian[87] in the gas phase and solution using a polarized continuum model.[91,92] The CIS and TD-DFT calculated vertical energies for local excitations (Table S4) deviate on average 3% from experimental values and resemble those of the individual building blocks.

Preliminary insights into excited-state interactions came from steady-state fluorescence measurements. Initially, the fluorescence of **24** was recorded upon 380 nm photoexcitation (Figure S3a) disclosing mostly C_{60} fluorescence at 710 nm. To reduce the background noise, a 450 nm optical filter

was used. Importantly, a marked bridge fluorescence quenching is seen. The filter partially blocks the signal stemming from the bridge, which is, however, not the main cause of the fluorescence quenching. The latter was confirmed in experiments without any filter. Despite the fact that the fluorescence quantum yield of **8** in THF is 0.62, no presence of any intensive signals was noted. Notably, 380 nm excitation directs the light nearly quantitatively to the bridge rather than to C_{60}. Still, the excitation spectrum strongly resembles the absorption spectrum of **24** (Figure S3b). It is safe to conclude that the C_{60} fluorescence evolves, to a large extent, from a singlet excited state energy transfer and, to minor extent, from direct excitation. To confirm hypothesis, electron-transfer contributions from the photoexcited bridge had to be ruled out. The almost constant (approximately 6×10^{-4}) fluorescence quantum yields of C_{60} in solvents of different polarity (Table S1) rule out any contribution from charge-transfer processes.[81,93] Upon excitation of reference compounds **15**-**17** at either 350 or 420 nm, mostly the ZnP fluorescence is observed, which remains constant regardless of the solvent polarity (Table S2). As the UV region of the absorption spectra is dominated by bridge features, an almost quantitative energy transfer from the bridge to ZnP is postulated upon 350 nm excitation (Figure S4a). Independent confirmation of this hypothesis was obtained from the excitation spectra, which clearly show that the ZnP fluorescence evolves from the bridge and ZnP (Figure S4b). The situation changes, however, upon inspection of the D–B–As **18**-**20**. In the case of **18** and **19**, the ZnP fluorescence is quenched by the presence of $C_{60,}$ which points to different deactivation pathways of the ZnP singlet excited state. Importantly, the use of more polar solvents such as THF (ε 7.60) (Figure 2) and PhCN (ε 24.8), enhances the fluorescence quenching relative to that seen for toluene (ε 2.38). Surprisingly, **20** does not follow this trend, as the ZnP fluorescence quantum yields remain nearly constant in toluene, THF, and PhCN (Table S2).

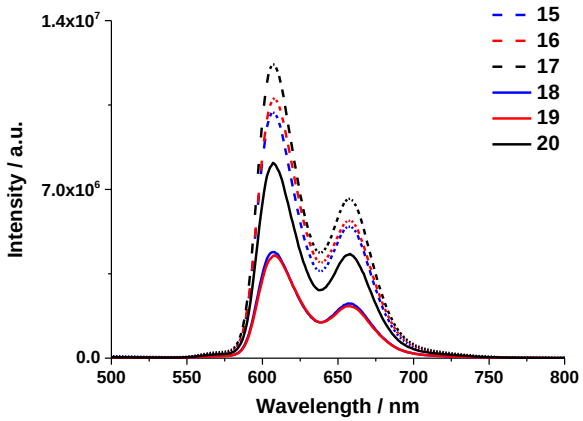

Figure 2. Room-temperature fluorescence spectra of **15-20** in THF upon 420 nm excitation with matching optical density.

Our observations suggest that incorporating S has a strong impact on the electronic communication between ZnP and C_{60}. The fluorescence lifetimes were determined. All ZnP fluorescence decays were best fitted by a single exponential decay (Table 2). Overall, an increase in solvent polarity leads to an acceleration of the fluorescence deactivation in **18** and **19**, while in **20** the lifetimes remain nearly constant.

Table 2. Fluorescence lifetimes (τ_{TCSPC}) upon 420 nm excitation in solvents of different polarity.

τ TCSPC / ns	Toluene	THF	PhCN
ZnP-Ph-Fl-S-CHO (**15**)	1.67	1.29	1.45
ZnP-Ph-S-Fl-CHO (**16**)	1.67	1.35	1.54
ZnP-Ph-Fl-S-Fl-CHO (**17**)	1.67	1.36	1.53
ZnP-Ph-Fl-S-C_{60} (**18**)	1.04	0.71	0.60
ZnP-Ph-S-Fl-C_{60} (**19**)	0.97	0.57	0.54
ZnP-Ph-Fl-S-Fl-C_{60} (**20**)	1.42	1.22	1.33

Complementary transient absorption measurements were performed to determine the nature of the deactivation pathways. Argon-saturated solutions of reference compounds **15-17** and D–B–As **18-20**

were photoexcited at either 387 or 430 nm. Despite the excitation of the bridges at 387 nm, no spectral evidence that would imply bridge-centered excited states was found in **15-17**. Instead, the differential spectra recorded directly after the excitation resemble the fingerprints of the ZnP singlet excited state.[94] In particular, transient features at 455 nm and between 580 and 750 nm are found. These decay biexponentially within approximately 1.3 ps and 1.6 ns and give rise to new transients at 468 and 840 nm in toluene. This implies first an internal conversion followed by an intersystem crossing (ISC) between the ZnP singlet locally excited state (2.16 eV) and the corresponding ZnP triplet state (1.53 eV) (Figure S5).

This picture is changed by the presence of C_{60} in **18** and **19**. Considering the light partitioning, which was derived from the extinction coefficients, between ZnP, C_{60}, and the bridge **23** (Figure S6a-b), which is 1:0.57:0.37 at the 387 nm excitation wavelength, different deactivation pathways are likely. Despite clear excitation of the bridges in **18** and **19**, no spectral evidence for bridge-centered singlet–singlet absorption features around 655 nm was found (Figure 3a and S6). This is supported by the results of the CIS calculations (SI). The predicted S1-SX transitions show oscillator strengths in the range of 0.1, 0.19, 0.20 and 0.35 for the porphyrin-centered vertical excitations predicted at 614 nm, 567 nm, 535 nm and 446 nm, respectively. In stark contrast, the bridge-centered S1-SX transition at 656 nm was predicted to have an oscillator strength of 0.002, which is only 1-2 % compared to those of the porphyrin.

a)

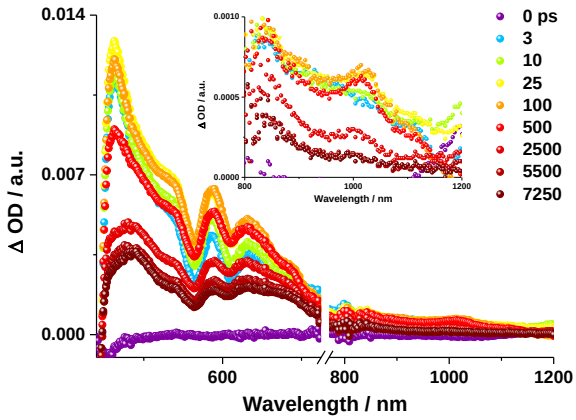

b)

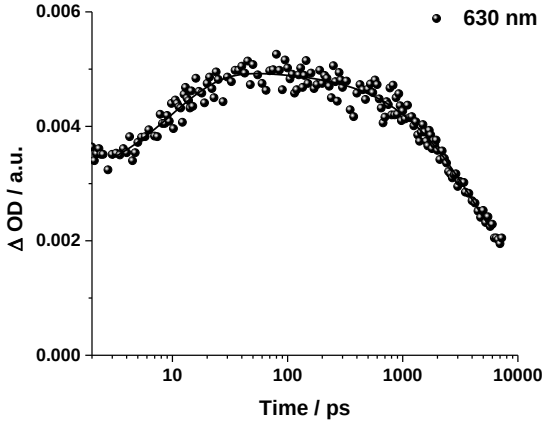

Figure 3. a) Differential absorption spectra (visible and near-infrared) obtained upon femtosecond flash photolysis (387 nm) of **19** in argon-saturated PhCN with several time delays between 0 and 7250 ps at room temperature. Inset shows the 800-1200 nm range for a better visualization of the C_{60} radical anion. b) Time absorption profile at 630 nm monitoring the charge separation and charge recombination dynamics.

Careful analysis of the absorption time profiles of **18** and **19** in THF revealed the presence of short-lived mono-exponential components with lifetimes of approximately 13 and 9 ps. Notably, the 9 ps component is not detected upon selective excitation of ZnP at 550 nm. This, together with the fact that the bridge fluorescence is quantitatively quenched, allows us to conclude that an energy transfer from the bridge to the lower lying ZnP singlet excited state takes place. In PhCN, the energy transfer is masked by solvent-related features. In PhCN and upon 387 nm excitation, new transients evolve at 630 and 1020 nm, which are attributed to the ZnP radical cation and C_{60} radical anion absorptions, respectively, as fingerprints of a charge-separated state. The charge-separation half-lives were fit monoexponentially and are 235 ± 68 ps for **18** and 232 ± 40 ps for **19**, while those for charge-recombination decay also monoexponentially within 2.1 ns for **18** and 2.8 ns and **19** (Figure 3b). Overall, an acceleration of the charge recombination upon increasing the solvent polarity was observed, which suggests that the dynamics are placed into the inverted region of the Marcus parabola[46,95] (Table 3, Figure S7). Careful analysis revealed only weak electronic coupling of 5.54 and 4.68 cm^{-1},

respectively, for **18** and **19**. In case of **20**, insights into electronic coupling were provided by analysis of the molecular frontier orbitals (Figure S16). The DFT calculations revealed important differences. In **18** and **19**, the HOMO is delocalized on the ZnP and the majority of the bridge. Whereas in **20**, the overlap of the frontier orbitals is less significant. The latter, in combination with the increasing separation of the HOMO and LUMO levels, indicates smaller electronic coupling in **20**.

All the kinetics following 430 nm excitation are collated in Table S3. Additionally, due to the direct excitation of ZnP and C_{60} at 387 nm, intersystem crossing to their triplet-excited states is observed. These were identified by long-lived triplet transitions at 486 nm for ZnP[94] and 684 nm for C_{60},[96] which are particularly pronounced on the μs scale measurements (Figure S8). Finally, fast formation of ZnP singlet excited state transients occurs upon excitation at 430 nm. The latter transform monoexponentially within 454 ± 64 ps for **18** and 389 ± 38 ps for **19** in THF, into the ZnP radical cation and C_{60} radical anion fingerprints. Similar to what has been seen upon 387 nm excitation, the long-lived triplet transitions of ZnP were observed (Figure S9).

Table 3. Charge-separation (k_{CS}) and -recombination (k_{CR}) rates upon 387 nm excitation.

	k_{CS} / s^{-1}		k_{CR} / s^{-1}	
	THF	PhCN	THF	PhCN
ZnP-Ph-Fl-S-C_{60} (**18**)	2.3×10^9	4.3×10^9	2.7×10^8	4.7×10^8
ZnP-Ph-S-Fl-C_{60} (**19**)	2.2×10^9	4.3×10^9	3.1×10^8	3.5×10^8
ZnP-Ph-Fl-S-Fl-C_{60} (**20**)	2.9×10^{10}	7.4×10^9	6.6×10^8	5.6×10^8

Transient absorption measurements with **20** were performed with 387 and 430 nm excitations analogously to **18** and **19 (**Figure S10). The results depend on the excitation wavelength. For an analogous conjugate without S, a charge-separated state with a 2000 ns lifetime was reported in PhCN upon 430 nm excitation.[41] In the present case, no evidence for the formation of any charge-separated state was found on photoexcitation at 430 nm. Instead, the spectral fingerprints of the ZnP singlet

excited-state decay within approximately 1.6 ns *via* intersystem crossing to afford the long-lived triplet excited state of ZnP (Figure S11). Upon 387 nm excitation, the transient absorption features resemble those of **18** and **19**. Considering our findings using 430 nm excitation, an electron transfer from the ZnP singlet excited state to the fullerene moiety can be ruled out.

Vertical excitations, based on the optimized ground-state geometries, were calculated (AM1*/CIS) for **18-20** with varying solvent polarity to study solvent effects on the excited states. These calculations also allowed us to analyze possible electron-trap states that hinder the direct electron transfer from the ZnP towards C_{60} for **20**. Relative to the gas phase, the charge-separated state energies (Table S5, Figure S12) are stabilized by over 1.0 eV for all compounds. However, the charge-separated state is better stabilized upon increasing the solvent polarity in **20** than in **18** and **19**. A possible rational lies in the different electron donor-acceptor distances: 26.7 Å (**18** and **19**) versus 33.6 Å (**20**), which also explains the higher dipole moment of the fully charge-separated state of **20**. In stark contrast to **18** and **19**, compound **20** exhibits a bridge-centered charge transfer state (Figure S13), which for non-polar solvent environments is energetically favored, compared to the fully charge-separated state (Figure 4).

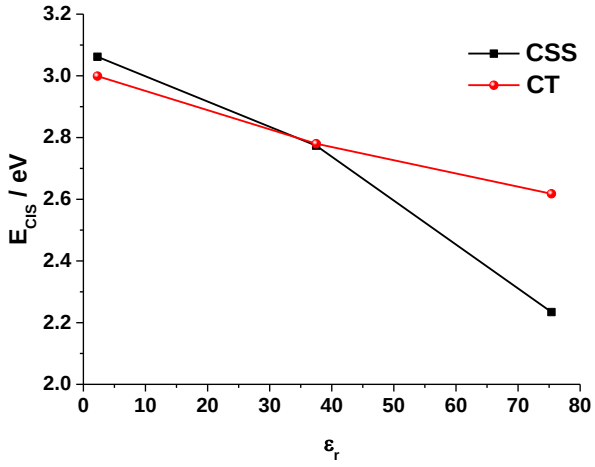

Figure 4. Calculated vertical excitation energies for the charge separated state (CSS, black) and the charge transfer state (CT, red) for **20** as a function of solvent polarity.

387 nm excitation leads to the simultaneous population of ZnP, C_{60} and bridge-centered singlet states in a 5:3:2 ratio (Figure 5). By virtue of the strong fluorescent nature of the reference compounds **15**-**17**, the following assignment is made for **20**. The 10 ps component relates to energy transfer from the bridge singlet excited (3.07 eV) to the ZnP second singlet excited state (2.95 eV) in THF, followed by a fast internal conversion to afford the ZnP first singlet excited state and ISC to the ZnP triplet excited state in 1.6 ns. This is in line with the 99.3% efficiency of Förster-type energy transfer for **17**, which was determined using fluorescence quantum yields of the bridge alone (compound **8**) and in **17**. Additionally, the experimental observations are in good agreement with the results of the CIS excited-state calculations, where a pronounced coupling between bridge-centered singlet excited state and ZnP second singlet excited state is observed for **18**-**20** (Figure 6 for **18**). Notably, transfer of singlet excited-state energy from the bridge to C_{60} is also feasible, shown for **24**: we also cannot exclude it in this case.

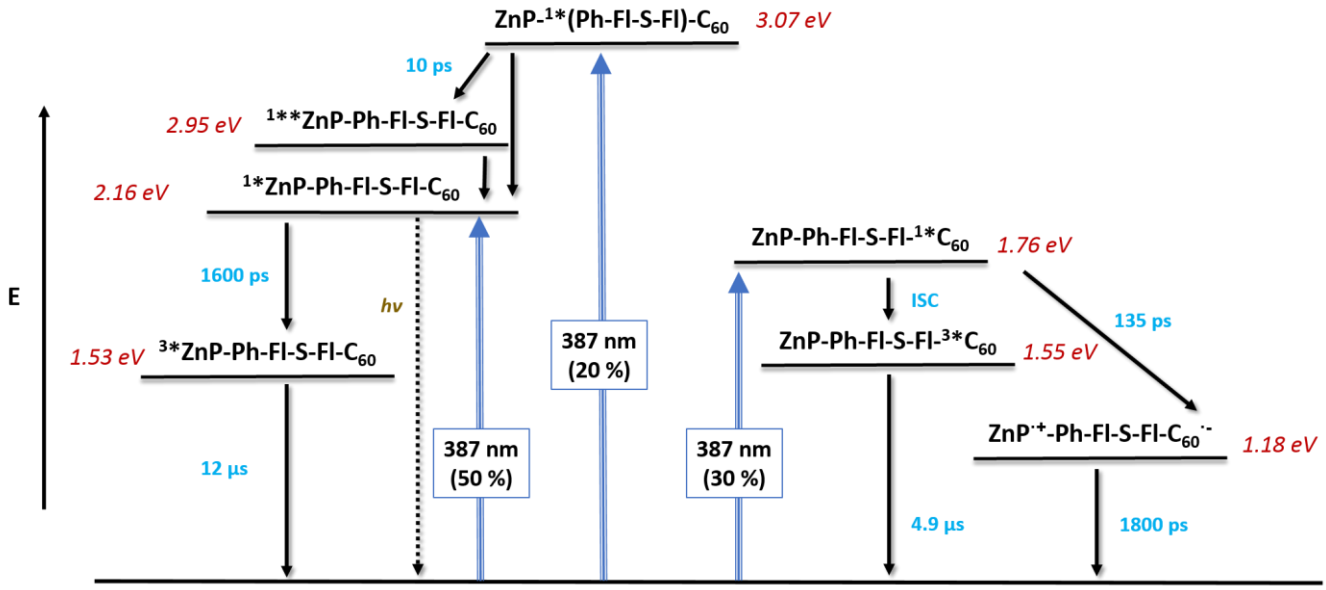

Figure 5. Energy level diagram of **20** reflecting the energetic pathways in PhCN after excitation at 387 nm. The dashed arrow refers to fluorescence emission, whereas black lines refer to nonradiative processes.

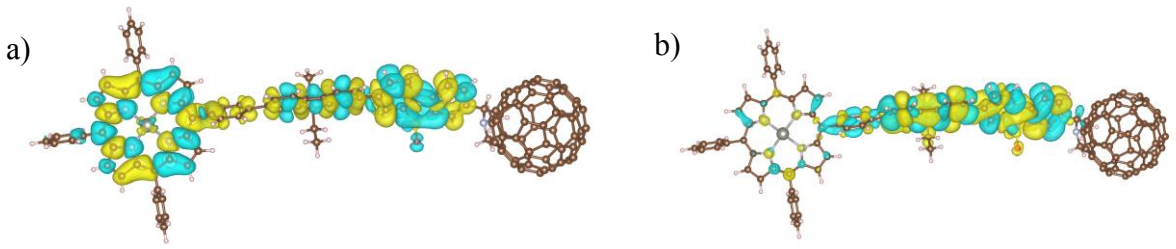

Figure 6. Spin densities of a) ZnP second singlet excited state (2.95 eV) and b) bridge-centered singlet excited state (3.19 eV) of **18** in the gas phase, based on AM1* CIS calculations.

The remaining 30% in the absorption cross section results in populating the fullerene excited singlet state and subsequently in a hole-transfer towards ZnP and within 135 ± 54 ps in PhCN (Figure 7). The 15% contribution of the 135 ps component to the fit was derived based on the amplitudes. The lifetime of the charge-separated state reaches 1.5 and 1.8 ns in THF and PhCN, respectively. The multiplicity of different processes made the analysis challenging. Still, the dynamics for charge separation and recombination were derived from bi-exponential fits in multiwavelength analyses.

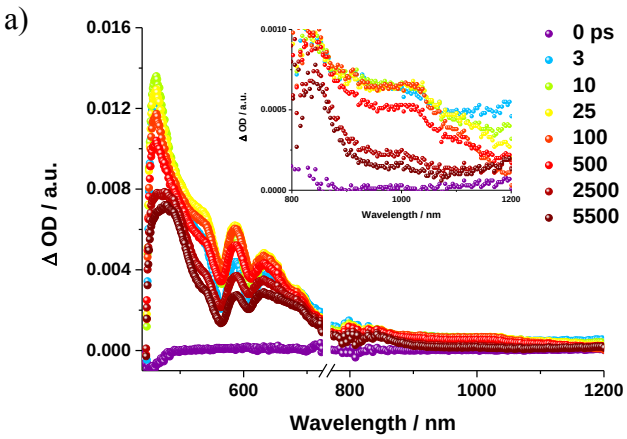

b)

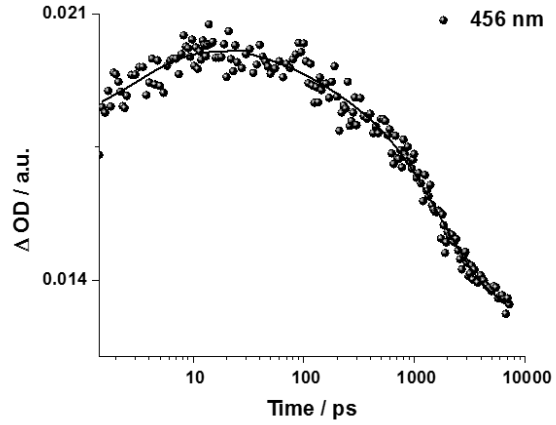

Figure 7. a) Differential absorption spectra (visible and near-infrared) obtained upon femtosecond flash photolysis (387 nm) of **20** in argon-saturated PhCN with several time delays between 0 and 5500 ps at room temperature. Inset shows the 800-1200 nm range for a better visualization of the C_{60} radical anion. b) Time absorption profile at 456 nm monitoring the charge separation dynamics.

In contrast to **18** and **19**, increasing the solvent polarity results in slower charger recombination dynamics. Likewise, in **18** and **19**, the formation of the triplet-excited features of ZnP and C_{60} is a consequence of the different light partitioning between ZnP, C_{60}, and the bridge **8** at the 387 nm excitation wavelength. This all suggests that **20** features a gating of charge transfer; incorporation of S suppresses electron-transfer from ZnP to C_{60}, but facilitates hole-transfer from C_{60} to ZnP.

Mechanistic Aspects. Temperature-dependent femtosecond transient absorption experiments were performed in the range between 280 and 355 K to shed light on the charge-transfer mechanism in D–B–As **18**-**20**. Importantly, no evidence for charge separation was found upon 430 nm excitation of **20** even in the high-temperature regime. Thus, the presence of S introduces a significant activation barrier for any electron-transfer, which cannot be overcome under the conditions applied. A temperature dependence can, however, be seen in Figure 8 with 387 nm laser excitation pulses. Within the framework of the Arrhenius formalism, the activation energies change from 0.016 to 0.093 eV for **20** on

going from the low to the high-temperature regime. We therefore postulate a change in charge-recombination mechanism, that is, coherent transport aided by superexchange *versus* hopping. In the cases of **18** and **19**, the activation energy remains constant at 0.021 and 0.010 eV, respectively, in the 387 nm excitation experiments.

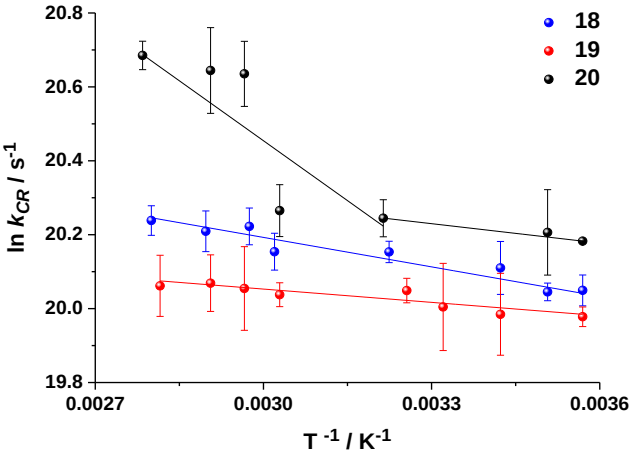

Figure 8. Temperature dependence of the charge recombination for **18-20** in the 280 to 355 K temperature regime based on the temperature-dependent femtosecond transient absorption experiments upon 387 nm excitation in PhCN.

Our calculations show that the energy gap between the lowest-lying ZnP and bridge-centered unoccupied orbitals are 0.34, 0.30 and 0.24 eV for **18**, **19** and **20**, respectively (Figure S14). Thus in combination with the bridge contribution to porphyrin and fullerene-centered MOs, a superexchange mechanism seems feasible when the ZnP excited states are populated in 430 nm excitation experiments. Relative to **18**, 100 meV lower relative energies of the lowest-lying bridge virtual orbital in **20** indicates that there should be energetically low-lying bridge-centered excited states, as found in the CIS calculations. The bridge-centered charge-transfer state with its higher electron density on the S unit and lower electron density on the Fl units constitutes a trap states for electrons. Considering that the charge-transfer state is bridge-centered with contributions exclusively from the Fl and S building blocks, it is hardly surprising that the transient absorption spectra reveal only ZnP characteristics.

Notably, the femtosecond transient absorption experiments described above exhibit no fingerprints of charge-separated states for **20** upon ZnP photoexcitation. This rules out possible electron-transfer activations. Interestingly the highest-lying bridge-centered occupied orbitals are destabilized with respect to the C_{60} HOMO by 27, 21, and 91 meV for **18**, **19**, and **20**, respectively. Importantly, because of the almost matching HOMOs of the electron-accepting C_{60} and the bridges, hole-transfer from C_{60} to ZnP is very likely in **18**-**20** upon excitation at 387 nm.

We hypothesize that the charge recombination mechanism in **18** and **19** involves contributions from both electron and hole-transfer. As observed for **18**, large energy gaps of approximately 1.15, 1.08, and 1.05 eV for **18**, **19**, and **20**, respectively, between the lowest-lying unoccupied orbitals of the C_{60} and the bridge should result in an exclusive electron-tunneling mechanism, as suggested by the temperature-dependence measurements. At the same time, the energy gaps of about 0.47, 0.45, and 0.38 eV for **18**, **19**, and **20**, respectively, between the highest occupied orbitals of the ZnP and the bridge imply a dominant role of the superexchange-assisted coherent mechanism for charge-recombination *via* hole-transfer.[97]

Conclusions

A new series of ZnP-wire-C_{60} conjugates (**18-20**), in which co-oligomer bridges incorporating both fluorenes (Fl) and dibenzothiophene-*S,S*-dioxides (S) are covalently linked to electron-donating ZnP and accepting C_{60}, has been synthesized and characterized. The special feature of these systems is that the position of the S units in the co-oligomer linker is systematically varied. In this way, the electronic coupling between the two electroactive terminal units, ZnP and C_{60}, has been tuned.

Only subtle effects in terms of charge transfer evolve when the S unit is placed either adjacent to ZnP (**19**) or C_{60} (**18**) as photoexcitation of either ZnP or C_{60} affords the efficient formation of a charge-separated state followed by a slower charge recombination. Both electron and hole-transfer are likely to be operative. In stark contrast, placing the S unit in the center of the bridge with one Fl unit adjacent to ZnP and one adjacent to C_{60} (**20**), either blocks or activates the charge-separated state formation on

photoexcitation of ZnP or C_{60}, respectively. In other words, unidirectional charge transfer is only possible for holes, but not for electrons because of the electron-withdrawing nature of the S unit. This also affects the charge recombination, which appears to be appreciably faster in **20** than in **18** or **19**.

Molecular-modeling studies corroborate the experimental results. This work establishes that dibenzothiophene-*S,S*-dioxide is an excellent electron-mediating subunit for incorporation in bridges of donor-bridge-acceptor systems and for probing how subtle electronic effects influence the photophysical properties of the arrays.

ACKNOWLEDGMENT. This work was supported by the EC FP7 ITN "MOLESCO" project no. 606728. We thank EPSRC (U.K.) grant EP/L0261X/1 for funding equipment used for the work in Durham. Work in Erlangen was supported by the "Solar Technologies go Hybrid" initiative of the Bavarian Ministry for Education, Culture and Science. This manuscript is dedicated to the memory of Professor Thomas Wandlowski.

Supporting Information: Synthetic details and characterization; electrochemical and photophysical data; theoretical details.

(1) Brabec, C. J.; Sariciftci, N. S.; Hummelen, J. C. Plastic Solar Cells. *Adv. Funct. Mater.* **2001**, *11*, 15-26.

(2) Coakley, K. M.; McGehee, M. D. Conjugated Polymer Photovoltaic Cells. *Chem. Mater.* **2004**, *16*, 4533-4542.

(3) Günes, S.; Neugebauer, H.; Sariciftci, N. S. Conjugated Polymer-Based Organic Solar Cells. *Chem. Rev.* **2007**, *107*, 1324-1338.

(4) Thompson, B. C.; Fréchet, J. M. J. Polymer-Fullerene Composite Solar Cells. *Angew. Chem. Int. Ed.* **2008**, *47*, 58-77.

(5) Dennler, G.; Scharber, M. C.; Brabec, C. J. Polymer-Fullerene Bulk-Heterojunction Solar Cells. *Adv. Mater.* **2009**, *21*, 1323-1338.

(6) Kippelen, B.; Brédas, J.-L. Organic Photovoltaics. *Energy Environ. Sci*. **2009**, *2*, 251-261.

(7) Delgado, J. L.; Bouit, P.-A.; Filippone, S.; Herranz, M. A.; Martín, N. Organic Photovoltaics: A Chemical Approach. *Chem. Commun*. **2010**, *46*, 4853-4865.

(8) The Special Issue on Organic Electronics. *Chem. Mater*. **2004**, *16*, 4381-4382.

(9) Organic Electronics and Optoelectronics. *Chem. Rev*. **2007**, *107*, 923-1386.

(10) Special Issue: Organic Electronics. *Isr. J. Chem*. **2014**, *54*, 413-835.

(11) Special Issue: Organic Electronics. *ChemPhysChem*. **2015**, *16*, 1097-1314.

(12) Parson, W. W. Electron Donors and Acceptors in the Initial Steps of Photosynthesis in Purple Bacteria: A Personal Account. *Photosynth. Res*. **2003**, *76*, 81-92.

(13) Wasielewski, M. R. Photoinduced Electron Transfer in Supramolecular Systems for Artificial Photosynthesis. *Chem. Rev*. **1992**, *92*, 435-461.

(14) Wasielewski, M. R. Energy, Charge, and Spin Transport in Molecules and Self-Assembled Nanostructures Inspired by Photosynthesis. *J. Org. Chem*. **2006**, *71*, 5051-5066.

(15) Kirner, S.; Sekita, M.; Guldi, D. M. 25th Anniversary Article: 25 Years of Fullerene Research in Electron Transfer Chemistry. *Adv. Mater*. **2014**, *26*, 1482-1493.

(16) Tour, J. M. Conjugated Macromolecules of Precise Length and Constitution. Organic Synthesis for the Construction of Nanoarchitectures. *Chem. Rev*. **1996**, *96*, 537-553.

(17) Shirota, Y. Organic Materials for Electronic and Optoelectronic Devices. *J. Mater. Chem*. **2000**, *10*, 1-25.

(18) Roncali, J. Oligothienylenevinylenes as a New Class of Multinanometer Linear π-Conjugated Systems for Micro- and Nanoelectronics. *Acc. Chem. Res*. **2000**, *33*, 147-156.

(19) Segura, J. L.; Martín, N. Functionalized Oligoarylenes as Building Blocks for New Organic Materials. *J. Mater. Chem*. **2000**, *10*, 2403-2435.

(20) Martín, N.; Sánchez, L.; Herranz, M. Á.; Illescas, B.; Guldi, D. M. Electronic Communication in Tetrathiafulvalene (TTF)/C60 Systems: Toward Molecular Solar Energy Conversion Materials?. *Acc. Chem. Res*. **2007**, *40*, 1015-1024.

(21) Wassel, R. A.; Gorman, C. B. Establishing the Molecular Basis for Molecular Electronics. *Angew. Chem. Int. Ed*. **2004**, *43*, 5120-5123.

(22) Carroll, R. L.; Gorman, C. B. The Genesis of Molecular Electronics. *Angew. Chem. Int. Ed*. **2002**, *41*, 4378-4400.

(23) Segura, J. L.; Martín, N.; Guldi, D. M. Materials for Organic Solar Cells: The C60/π-Conjugated Oligomer Approach. *Chem. Soc. Rev*. **2005**, *34*, 31-47.

(24) Schubert, C.; Margraf, J. T.; Clark, T.; Guldi, D. M. Molecular Wires – Impact of π-Conjugation and Implementation of Molecular Bottlenecks. *Chem. Soc. Rev*. **2015**, *44*, 988-998.

(25) de Cola, L. (editor) *Top. Curr. Chem.* Springer, Berlin Heidelberg, **2005**, *275,* 63-103.

(26) Molina-Ontoria, A.;Wielopolski, M.; Gebhardt, J.; Gouloumis, A.; Clark, T.; Guldi, D. M.; Martín, N. [2,2′]Paracyclophane-Based π-Conjugated Molecular Wires Reveal Molecular-Junction Behavior. *J. Am. Chem. Soc.* **2011**, *133*, 2370-2373.

(27) Davis, W. B.; Ratner, M. A.; Wasielewski, M. R. Conformational Gating of Long Distance Electron Transfer through Wire-like Bridges in Donor-Bridge-Acceptor Molecules. *J. Am. Chem. Soc.* **2001**, *123*, 7877-7886.

(28) van Hal, P. A.; Meskers, S. C. J.; Janssen, R. A. J. Photoinduced Energy and Electron Transfer in Oligo(p-Phenylene Vinylene)-Fullerene Dyads. *Appl. Phys. A: Mater. Sci. Process* **2004**, *79*, 41-46.

(29) de la Torre, G.; Giacalone, F.; Segura, J. L.; Martín, N.; Guldi, D. M. Electronic Communication through π -Conjugated Wires in Covalently Linked Porphyrin/C60 Ensembles. *Chem. Eur. J*. **2005**, *11*, 1267-1280.

(30) Figueira-Duarte, T. M.; Gégout, A.; Nierengarten, J.-F. Molecular and Supramolecular C60–Oligophenylenevinylene Conjugates. *Chem. Commun*. **2007**, 109-119.

(31) Toivonen, T. L. J.; Hukka, T. I. A Density Functional Theory (DFT) and Time-Dependent Density Functional Theory (TDDFT) Study on Optical Transitions in Oligo(p-Phenylenevinylene)−Fullerene Dyads and the Applicability to Resonant Energy Transfer. *J. Phys. Chem. A* **2007**, *111*, 4821-4828.

(32) Santos, J.; Illescas, B. M.; Wielopolski, M.; Silva, A. M. G.; Tomé, A. C.; Guldi, D. M.; Martín, N. Efficient Electron Transfer in β-Substituted Porphyrin-C60 Dyads Connected through a p-Phenylenevinylene Dimer. *Tetrahedron* **2008**, *64*, 11404-11408.

(33) Nierengarten, J.-F.; Gu, T.; Aernouts, T.; Greens, W.; Poortmans, J.; Hadziioannou, G.; Tsamouras, D. Fullerene–Oligophenyleneethynylene Conjugates: Relationships between Charge-Carrier Mobility, Photovoltaic Characteristics and Chemical Structure. *Appl. Phys. A: Mater. Sci. Process* **2004**, *79*, 47-49.

(34) Koynov, K.; Bahtiar, A.; Bubeck, C.; Mühling, B.; Meier, H. Effect of Donor-Acceptor Substitution on the Nonlinear Optical Properties of Oligo(1,4-Phenyleneethynylene)s Studied by Third Harmonic Generation Spectroscopy. *J. Phys. Chem. B* **2005**, *109*, 10184-10188.

(35) Zhao, Y.; Shirai,Y.; Slepkov, A. D.; Cheng, L.; Alemany, L. B.; Sasaki, T.; Hegmann, F. A.; Tour, J. M. Synthesis, Spectroscopic and Nonlinear Optical Properties of Multiple [60]Fullerene–Oligo(p-Phenylene Ethynylene) Hybrids. *Chem. Eur. J.* **2005**, *11*, 3643-3658.

(36) Fortage, J.; Göransonn, E.; Blart, E.; Becker, H.-C.; Hammarström, L.; Odobel, F. Strongly Coupled Zinc Phthalocyanine–Tin Porphyrin Dyad Performing Ultra-Fast Single Step Charge Separation over a 34 Å distance. *Chem. Commun*. **2007**, 4629-4631.

(37) Pu, K.-Y.; Qi, X.-Y.; Yang, Y. -L.; Lu, X.-M.; Li, T.-C.; Fan, Q.-L.; Wang, C.; Liu, B.; Chan, H. S. O.; Huang, W. Supramolecule-Regulated Photophysics of Oligo(p-Phenyleneethynylene)- Based Rod–Coil Block Copolymers: Effect of Molecular Architecture. *Chem. Eur. J*. **2008**, *14*, 1205-1215.

(38) Lembo, A.; Tagliatesta, P.; Guldi, D. M.; Wielopolski, M.; Nuccetelli, M. Porphyrin-β-Oligo-Ethynylenephenylene-[60]Fullerene Triads: Synthesis and Electrochemical and Photophysical

Characterization of the New Porphyrin-Oligo-PPE-[60]Fullerene Systems. *J. Phys. Chem. A* **2009**, *113*, 1779-1793.

(39) Linton, K. E.; Fox, M. A.; Pålsson, L.-O.; Bryce, M. R. Oligo(p-Phenyleneethynylene) (OPE) Molecular Wires: Synthesis and Length Dependence of Photoinduced Charge Transfer in OPEs with Triarylamine and Diaryloxadiazole End Groups. *Chem. Eur. J.* **2015**, *21*, 3997-4007.

(40) Atienza-Castellanos, C.; Wielopolski, M.; Guldi, D. M.; van der Pol, C.; Bryce, M. R.; Filippone, S.; Martín, N. Determination of the Attenuation Factor in Fluorene-Based Molecular Wires. *Chem. Commun*. **2007**, 5164-5166.

(41) Wielopolski, M.; de Miguel Rojas, G.; van der Pol, C.; Brinkhaus, L.; Katsukis, G.; Bryce, M. R.; Clark, T.; Guldi, D. M. Control over Charge Transfer through Molecular Wires by Temperature and Chemical Structure Modifications. *ACS Nano* **2010**, *4,* 6449-6462.

(42) Walther, M. E.; Grilj, J.; Hanss, D.; Vauthey, E.; Wenger, O. S. Photoinduced Processes in Fluorene-Bridged Rhenium–Phenothiazine Dyads – Comparison of Electron Transfer Across Fluorene, Phenylene, and Xylene Bridges. *Eur. J. Inorg. Chem*. **2010**, 4843-4850.

(43) Schubert, C.; Wielopolski, M.; Mewes, L.-H.; de Miguel Rojas, G.; van der Pol, C.; Moss, K. C.; Bryce, M. R.; Moser, J. E.; Clark, T.; Guldi, D. M. Precise Control of Intramolecular Charge-Transport: The Interplay of Distance and Conformational Effects. *Chem. Eur. J*. **2013**, *19*, 7575-7586.

(44) Wielopolski, M.; Santos, J.; Illescas, B. M.; Ortiz, A.; Insuasty, B.; Bauer, T.; Clark, T.; Guldi, D. M.; Martín, N. Vinyl Spacers-Tuning Electron Transfer through Fluorene-Based Molecular Wires. *Energy Eviron. Sci.* **2011**, *4,* 765-771.

(45) Sukegawa, J.; Schubert, C.; Zhu, X.; Tsuji, H.; Guldi, D. M.; Nakamura, E. Electron Transfer through Rigid Organic Molecular Wires Enhanced by Electronic and Electron–Vibration Coupling. *Nature Chem.* **2014**, *6*, 899-905.

(46) Vail, S. A.; Krawczuk, P. J.; Guldi, D. M.; Palkar, A.; Echegoyen, L.; Tomé, J. P. C.; Fazio, M. A.; Schuster, D. I. Energy and Electron Transfer in Polyacetylene-Linked Zinc–Porphyrin-[60]Fullerene Molecular Wires. *Chem. Eur. J.* **2005**, *11*, 3375-3388.

(47) Vail, S. A.; Schuster, D. I.; Guldi, D. M.; Isosomppi, M.; Tkachenko, N.; Lemmetyinen, H.; Palkar, A.; Echegoyen, L.; Chen, X.; Zhang, J. Z. H. Energy and Electron Transfer in β-Alkynyl-Linked Porphyrin−[60]Fullerene Dyads. *J. Phys. Chem. B* **2006**, *110*, 14155-14166.

(48) Wang, C.; Pålsson, L. -O.; Batsanov, A. S.; Bryce, M. R. Molecular Wires Comprising π-Extended Ethynyl- and Butadiynyl-2,5-Diphenyl-1,3,4-Oxadiazole Derivatives: Synthesis, Redox, Structural, and Optoelectronic Properties. *J. Am. Chem. Soc*. **2006**, *128*, 3789-3799.

(49) Pålsson, L.-O.; Wang, C.; Batsanov, A. S.; King, S. M.; Beeby, A.; Monkman, A. P.; Bryce, M. R. Efficient Intramolecular Charge Transfer in Oligoyne-Linked Donor– π–Acceptor Molecules. *Chem.-Eur. J.* **2010**, *16*, 1470-1479.

(50) Nakamura, T.; Fujitsuka, M.; Araki, Y.; Ito, O.; Ikemoto, J.; Takimiya, K.; Aso, Y.; Otsubo, T. Photoinduced Electron Transfer in Porphyrin-Oligothiophene-Fullerene Linked Triads by Excitation of a Porphyrin Moiety. *J. Phys. Chem. B* **2004**, *108*, 10700-10710.

(51) Huang, C.-H.; McClenaghan, N. D.; Kuhn, A.; Hofstraat, J. W.; Bassani, D. M. Enhanced Photovoltaic Response in Hydrogen-Bonded All-Organic Devices. *Org. Lett*. **2005**, *7*, 3409-3412.

(52) Petrella, A.; Cremer, J.; de Cola, L.; Bäuerle, P.; Williams, R. M. Charge Transfer Processes in Conjugated Triarylamine-Oligothiophene-Perylenemonoimide Dendrimers. *J. Phys. Chem. A* **2005**, *109*, 11687-11695.

(53) Narutaki, M.; Takimiya, K.; Otsubo, T.; Harima, Y.; Zhang, H.; Araki, Y.; Osamu, I. Synthesis and Photophysical Properties of Two Dual Oligothiophene-Fullerene Linkage Molecules as Photoinduced Long-Distance Charge Separation Systems. *J. Org. Chem*. **2006**, *71*, 1761-1768.

(54) Oswald, F.; Islam, D.-M. S.; Araki, Y.; Troiani, V.; Caballero, R.; de la Cruz, P.; Ito, O.; Langa, F. High Effectiveness of Oligothienylenevinylene as Molecular Wires in Zn-porphyrin and C60 Connected Systems. *Chem. Commun*. **2007**, 4498-4500.

(55) Winters, M. U.; Dahlstedt, E.; Blades, H. E.; Wilson, C. J.; Frampton, M. J.; Anderson, H. L.; Albinsson, B. Probing the Efficiency of Electron Transfer through Porphyrin-Based Molecular Wires. *J. Am. Chem. Soc*. **2007**, *129*, 4291-4297.

(56) Barigelletti, F.; Flamigni, L.; Guardigli, M.; Juris, A.; Beley, M.; Chodorowski-Kimmes, S.; Collin, J.-P.; Sauvage, J.-P. Energy Transfer in Rigid Ru(II)/Os(II) Dinuclear Complexes with Biscyclometalating Bridging Ligands Containing a Variable Number of Phenylene Units. *Inorg. Chem*. **1996**, *35*, 136-142.

(57) Berresheim, A. J.; Müller, M.; Müllen, K. Polyphenylene Nanostructures. *Chem. Rev.***1999**, *99*, 1747-1786.

(58) Schlicke, B.; Belser, P.; de Cola, L.; Sabbioni, E.; Balzani, V. Photonic Wires of Nanometric Dimensions. Electronic Energy Transfer in Rigid Rodlike $Ru(bpy)_3^{2+}$-$(ph)_n$-$Os(bpy)_3^{2+}$ Compounds (ph = 1,4-Phenylene; n = 3, 5, 7). *J. Am. Chem. Soc*. **1999**, *121*, 4207-4214.

(59) Helms, A.; Heiler, D.; McLendon, G. Electron Transfer in Bis-Porphyrin Donor-Acceptor Compounds with Polyphenylene Spacers Shows a Weak Distance Dependence. *J. Am. Chem. Soc*. **1992**, *114*, 6227-6238.

(60) Cohen, R.; Stokbro, K.; Martin, J. M. L.; Ratner, M. A. Charge Transport in Conjugated Aromatic Molecular Junctions: Molecular Conjugation and Molecule-Electrode Coupling. *J. Phys. Chem. C* **2007**, *111*, 14893-14902.

(61) Weiss, E. A.; Wasielewski, M. R.; Ratner, M. A. Molecules as Wires: Molecule-Assisted Movement of Charge and Energy. *Top. Curr. Chem*. **2005**, *257*, 103-133.

(62) Guldi, D. M.; Illescas, B. M.; Atienza, C. M.; Wielopolski, M.; Martín, N. Fullerene for Organic Electronics. *Chem. Soc. Rev*. **2009**, *38*, 1587-1597.

(63) Eng, M. P.; Albinsson, B. Non-Exponential Distance Dependence of Bridge-Mediated Electronic Coupling. *Angew. Chem. Int. Ed*. **2006**, *45*, 5626-5629.

(64) Goldsmith, R. H.; Sinks, L. E.; Kelley, R. F.; Betzen, L. J.; Liu, W.; Weiss, E. A.; Ratner, M. A.; Wasielewski, M. R., Wire-like Charge Transport at near Constant Bridge Energy through Fluorene Oligomers. *Proc. Natl. Acad. Sci. U.S.A.* **2005**, *102*, 3540-3545.

(65) Mori, D.; Benten, H.; Ohkita, H.; Ito, S. Morphology-Limited Free Carrier Generation in Donor/Acceptor Polymer Blend Solar Cells Composed of Poly(3-Hexylthiophene) and Fluorene-Based Copolymer. *Adv. Energy Mater*. **2015**, *5*, Art. No. 1500304.

(66) Wang, X.; Wang, K.; Wang, M. Synthesis of Conjugated Polymers via an Exclusive Direct-Arylation Coupling Reaction: A Facile and Straightforward Way to Synthesize Thiophene-Flanked Benzothiadiazole Derivatives and Their Copolymers. *Polym. Chem*. **2015**, *6*, 1846-1855.

(67) Fratiloiu, S.; Fonseca, S. M.; Grozema, F. C.; Burrows, H. D.; Costa, M. L.; Charas, A.; Morgado, J.; Siebbeles, L. D. A. Opto-Electronic Properties of Fluorene-Based Derivatives as Precursors for Light-Emitting Diodes. *J. Phys. Chem. C* **2007**, *111*, 5812-5820.

(68) Perepichka, I. I.; Perepichka, I. F.; Bryce, M. R.; Pålsson, L.-O. Dibenzothiophene-S,S-Dioxide–Fluorene Co-Oligomers. Stable, Highly-Efficient Blue Emitters with Improved Electron Affinity. *Chem. Commun*. **2005**, 3397-3399.

(69) Dias, F. B.; Pollock, S.; Hedley, G.; Pålsson, L.-O.; Monkman, A.; Perepichka, I. I.; Perepichka, I. F.; Tavasli, M.; Bryce, M. R. Intramolecular Charge Transfer Assisted by Conformational Changes in the Excited State of Fluorene-Dibenzothiophene-S,S-Dioxide Co-Oligomers. *J. Phys. Chem. B* **2006**, *110*, 19329-19339.

(70) Li, H.; Batsanov, A. S.; Moss, K. C.; Vaughan, H. L.; Dias, F. B.; Kamtekar, K. T.; Bryce, M. R.; Monkman, A. P. The Interplay of Conformation and Photophysical Properties in Deep-Blue Fluorescent Oligomers. *Chem. Commun*. **2010**, *46*, 4812-4814.

(71) Cook, J. H.; Santos, J.; Li, H.; Al-Attar, H. A.; Bryce, M. R.; Monkman, A. P. Efficient Deep Blue Fluorescent Polymer Light-Emitting Diodes (PLEDs). *J. Mater. Chem. C* **2014**, *2*, 5587-5592.

(72) Yang, Y.; Yu, L.; Xue, Y.; Zou, Q.; Zhang, B.; Ying, L.; Yang, W.; Peng, J.; Cao, Y. Improved Electroluminescence Efficiency of Polyfluorenes by Simultaneously Incorporating Dibenzothiophene-S,S-Dioxide Unit in Main Chain and Oxadiazole Moiety in Side Chain. *Polymer* **2014**, 55, 1698-1706.

(73) Liu, J.; Zou, J.; Yang, W.; Wu, H.; Li, C.; Zhang, B.; Peng, J.; Cao, Y. Highly Efficient and Spectrally Stable Blue-Light-Emitting Polyfluorenes Containing a Dibenzothiophene-S,S-Dioxide Unit. *Chem. Mater*. **2008**, *20*, 4499-4506.

(74) Yu, L.; Liu, J.; Hu, S.; He, R.; Yang, W.; Wu, H.; Peng, J.; Xia, R.; Bradley, D. D. C. Red, Green, and Blue Light-Emitting Polyfluorenes Containing a Dibenzothiophene- S,S -Dioxide Unit and Efficient High-Color-Rendering-Index White-Light-Emitting Diodes Made Therefrom. *Adv. Funct. Mater*. **2013**, *23*, 4366-4376.

(75) Lorbach, A.; Hübner, A.; Wagner, M. Aryl(hydro)boranes: Versatile Building Blocks for Boron-Doped π-Electron Materials. *Dalton Trans.* **2012**, *41,* 6048-6063.

(76) Dou, C.; Ding, Z.; Zhang, Z.; Xie, Z.; Liu, J.; Wang, L. Developing Conjugated Polymers with High Electron Affinity by Replacing a C-C Unit with a B←N Unit. *Angew. Chem. Int. Ed.* **2015**, *54*, 3648-3652.

(77) de Miguel, G.; Wielopolski, M.; Schuster, D. I.; Fazio, M. A.; Lee, O. P.; Haley, C. K.; Ortiz, A. L.; Echegoyen, L.; Clark, T.; Guldi, D. M. Triazole Bridges as Versatile Linkers in Electron Donor–Acceptor Conjugates. *J. Am. Chem. Soc*. **2011**, *133*, 13036-13054.

(78) Lebedeva, M. A.; Chamberlain, T. W.; Khlobystov, A. N. Harnessing the Synergistic and Complementary Properties of Fullerene and Transition-Metal Compounds for Nanomaterial Applications. *Chem. Rev*. **2015**, *115*, 11301-11351.

(79) Dolman, S. J.; Gosselin, F.; O'Shea, P. D.; Davies, I. W. Selective Metal-Halogen Exchange of 4,4'-Dibromobiphenyl Mediated by Lithium Tributylmagnesiate. *Tetrahedron* **2006**, *62*, 5092-5098.

(80) Guo, Z.-S.; Zhao, L.; Pei, J.; Zhou, Z.-L.; Gibson, G.; Brug, J.; Lam, S.; Mao, S. S. CdSe/ZnS Nanoparticle Composites with Amine-Functionalized Polyfluorene Derivatives for Polymeric Light-Emitting Diodes: Synthesis, Photophysical Properties, and the Electroluminescent Performance. *Macromolecules* **2010**, *43*, 1860-1866.

(81) van der Pol, C.; Bryce, M. R.; Wielopolski, M.; Atienza-Castellanos, C.; Guldi, D. M.; Filippone, S.; Martín, N. Energy Transfer in Oligofluorene-C60 and C60-Oligofluorene-C60 Donor-Acceptor Conjugates. *J. Org. Chem*. **2007**, *72*, 6662-6671.

(82) Prato, M.; Maggini, M. Fulleropyrrolidines: A Family of Full-Fledged Fullerene Derivatives *Acc. Chem. Res.* **1998**, *31*, 519-526.

(83) Maggini, M.; Scorrano, G.; Prato, M. Addition of Azomethine Ylides to C60: Synthesis, Characterization, and Functionalization of Fullerene Pyrrolidines. *J. Am. Chem. Soc.* **1993**, *115*, 9798-9799.

(84) Becke, A. D. Density-Functional Thermochemistry. III. The Role of Exact Exchange. *J. Chem. Phys.* **1993**, *98*, 5648-5652.

(85) Dunning, T. H. Jr. Gaussian Basis Sets for Use in Correlated Molecular Calculations. I. The Atoms Boron through Neon and Hydrogen. *J. Chem. Phys.* **1989**, *90*, 1007-1023.

(86) Clark, T. The Local Electron Affinity for Non-Minimal Basis Sets. *J. Mol. Model.* **2010**, *16*, 1231-1238.

(87) Winget, P.; Horn, A. H. C.; Selçuki, C.; Martin, B.; Clark, T. AM1* Parameters for Phosphorus, Sulfur and Chlorine. *J. Mol. Model.* **2003**, *9*, 408-414.

(88) Atienza, C.; Martín, N.; Wielopolski, M.; Haworth, N.; Clark, T.; Guldi, D. M. Tuning Electron Transfer through p-Phenyleneethynylene Molecular Wires. *Chem. Commun.* **2006**, 3202-3204.

(89) Bauernschmitt, R.; Ahlrichs, R. Treatment of Electronic Excitations within the Adiabatic Approximation of Time Dependent Density Functional Theory. *Chem. Phys. Lett.* **1996**, *256*, 454-464.

(90) Casida, M. E.; Jamorski, C.; Casida, K. C.; Salahub, D. R. Molecular Excitation Energies to High-Lying Bound States from Time-Dependent Density-Functional Response Theory: Characterization and Correction of the Time-Dependent Local Density Approximation Ionization Threshold. *J. Chem. Phys.* **1998**, *108*, 4439-4449.

(91) Rauhut, G.; Clark, T.; Steinke, T. A Numerical Self-Consistent Reaction Field (SCRF) Model for Ground and Excited States in NDDO-Based Methods. *J. Am. Chem. Soc.* **1993**, *115*, 9174-9181.

(92) Gedeck, P.; Schneider, S. Numerical Self-Consistent Reaction Field Study of Intramolecular Charge Transfer in p-(Dimethylamino)-Benzonitrile. *J. Photochem. Photobiol. A: Chem.* **1997**, *105*, 165-181.

(93) Li, H.; Schubert, C.; Dral, P. O.; Costa, R. D.; La Rosa, A.; Thüring, J.; Liu, S.-X.; Yi, C.; Filippone, S.; Martín, N.; et al. Probing Charge Transfer in Benzodifuran-C_{60} Dumbbell-Type Electron Donor-Acceptor Conjugates: Ground- and Excited-State Assays. *ChemPhysChem*, **2013**, *14*, 2910-2919.

(94) Rodriguez, J.; Kirmaier, C.; Holten, D., Optical Properties of Metalloporphyrin Excited States. *J. Am. Chem. Soc.* **1989**, *111*, 6500-6506.

(95) Schuster, D. I.; Cheng, P.; Jarowski, P. D.; Guldi, D. M.; Luo, C.; Echegoyen, L.; Pyo, S.; Holzwarth, A. R.; Braslavsky, S. E.; Williams, R. M.; et al. Design, Synthesis, and Photophysical Studies of a Porphyrin-Fullerene Dyad with Parachute Topology; Charge Recombination in the Marcus Inverted Region. *J. Am. Chem. Soc.* **2004**, *126*, 7257-7270.

(96) Guldi, D. M.; Prato, M. Excited-State Properties of C_{60} Fullerene Derivatives. *Acc. Chem. Res.* **2000**, *33*, 695-703.

(97) Martín, N.; Giacalone, F.; Segura, J. L.; Guldi, D. M. Mimicking Photosynthesis: Covalent [60]Fullerene-Based Donor–Acceptor Ensembles. *Synth. Met.* **2004**, *147*, 57-61.

ToC Graphic